Structure prediction based on *ab initio* simulated annealing for boron nitride

K. Doll, J. C. Schön, and M. Jansen
Max Planck Institute for Solid State Research, Heisenbergstrasse 1, D-70569 Stuttgart, Germany
(Received 29 May 2008; revised manuscript received 2 September 2008; published 29 October 2008)

Possible crystalline modifications of chemical compounds at low temperatures correspond to local minima of the energy landscape. Determining these minima via simulated annealing is one method for the prediction of crystal structures, where the number of atoms per unit cell is the only information used. It is demonstrated that this method can be applied to covalent systems, such as boron nitride, using *ab initio* energies in all stages of the optimization, i.e., both during the global search and the subsequent local optimization. Ten low-lying structure candidates are presented, including both layered structures and three-dimensional network structures such as the wurtzite and zinc-blende types as well as a structure corresponding to the β-BeO-type.

DOI: 10.1103/PhysRevB.78.144110 PACS number(s): 61.50.Ah, 71.15.Nc, 61.66.Fn

I. INTRODUCTION

The knowledge about the crystal structure of a solid compound is one of the basic questions in solid-state theory.[1–5] Since the early 1990s, an effort has been made to develop methods to predict structures of solids without any experimental information about the structure. The starting point is the realization that any (meta)stable modification of a (solid) compound corresponds to a locally ergodic region on the energy landscape of the chemical system. For low temperatures, such regions are centered on the local minima of the energy that are surrounded by sufficiently high-energy barriers. Since both the thermodynamically stable and the multitude of kinetically stable modifications are of interest, the global search is not restricted to the determination of the global minimum, but it includes local minima.[4]

The most common methods used for the structure prediction of solids are simulated annealing,[6–8] genetic algorithms,[9–12] basin hopping,[13,14] or the recently introduced metadynamics.[15] Structure prediction usually involves a huge amount of CPU time, and therefore, efficient ways to keep the calculations tractable have to be found. Thus, the procedures were initially split in two steps: a global search on the potential surface was performed. The energy was evaluated with empirical potentials, e.g., Coulomb and Lennard-Jones potentials, or chemically or physically motivated cost functions. After the global search, e.g., using simulated annealing, possible structure candidates were locally optimized on the *ab initio* level, usually with density-functional theory.

Empirical potentials are very efficient but also have various drawbacks: they work reasonably well for ionic systems but less for covalent systems and some knowledge about the expected bond type is required in advance to choose the potential. Recently,[16] we demonstrated that a full *ab initio* treatment is feasible in both stages, i.e., the global search and the subsequent local optimization can both be performed on the *ab initio* level. The system considered (lithium fluoride) was chosen for several reasons: the small number of electrons leads to fast calculations and the ionicity of the system makes convergence easy. Moreover, the system had earlier been studied with model potentials,[17,18] and it turned out that the relevant minima were the same when full *ab initio* structure prediction was performed[16] (for a brief summary see also Ref. 19).

In the present work, boron nitride (BN) was chosen as an example for a covalent system. This is a significant extension of the previous work, since a covalent system is much more difficult to study: covalent bonds between the atoms have to be formed, and convergence for random structures is much more difficult in this case. At zero pressure, BN has a hexagonal structure with space group 194—see, e.g., Ref. 20. Under pressure, it may transform to a zinc-blende[21] or a wurtzite structure,[22] and a corresponding phase diagram was obtained.[23] There is, however, an ongoing discussion concerning the correct phase diagram—see, e.g., Ref. 24. Also, a rhombohedral structure was found (a layered structure similar to the hexagonal structure),[25] and turbostratic boron nitride with a random arrangement of the layers has been reported.[26] These structures are summarized in Table I. For overviews, see also Refs. 27 and 28. Early *ab initio* calculations were performed from the mid–1980s onward, e.g., Refs. 29–37.

The present task is (for several reasons) far from being straightforward: first, the CPU time has to be reduced by a large factor. As we showed for the LiF system,[16] simply performing simulated annealing with standard *ab initio* calculations would lead to CPU times of the order of two years for a single run and often hundreds of such runs need to be performed. Therefore, very subtle methods have to be employed to reduce the CPU time for the *ab initio* calculations

TABLE I. The experimentally found structures.

Structure type	Cell parameters and fractional coordinates
Hexagonal BN (Ref. 20)	a=2.504 Å, c=6.661 Å
	B (1/3, 2/3, 1/4)
	N (1/3, 2/3, 3/4)
Zinc blende (Ref. 21)	a=3.615 Å
	B (0, 0, 0)
	N (1/4, 1/4, 1/4)
Wurtzite (Ref. 22)	a=2.55 Å, c=4.20 Å
Rhombohedral (Ref. 25)	a=2.52 Å, c=10.02 Å

TABLE II. Basis sets used for the global search (I and II) and the local optimization (III).

Basis set I		Basis set II		Basis set III	
Exponent	Contraction	Exponent	Contraction	Exponent	Contraction
			B		
			s		
2.082×10^{3}	1.850×10^{-3}	2.082×10^{3}	1.850×10^{-3}	2.082×10^{3}	1.850×10^{-3}
3.123×10^{2}	1.413×10^{-2}	3.123×10^{2}	1.413×10^{-2}	3.123×10^{2}	1.413×10^{-2}
7.089×10^{1}	6.927×10^{-2}	7.089×10^{1}	6.927×10^{-2}	7.089×10^{1}	6.927×10^{-2}
1.985×10^{1}	2.324×10^{-1}	1.985×10^{1}	2.324×10^{-1}	1.985×10^{1}	2.324×10^{-1}
6.292×10^{0}	4.702×10^{-1}	6.292×10^{0}	4.702×10^{-1}	6.292×10^{0}	4.702×10^{-1}
2.129×10^{0}	3.603×10^{-1}	2.129×10^{0}	3.603×10^{-1}	2.129×10^{0}	3.603×10^{-1}
			sp		
2.282×10^{0}	-3.687×10^{-1}, 2.312×10^{-1}	2.282×10^{0}	-3.687×10^{-1}, 2.312×10^{-1}	2.282×10^{0}	-3.687×10^{-1}, 2.312×10^{-1}
—		4.652×10^{-1}	1.199×10^{0}, 8.668×10^{-1}	4.652×10^{-1}	1.199×10^{0}, 8.668×10^{-1}
			sp		
0.4	1.0, 1.0	0.25	1.0, 1.0	0.197	1.0, 1.0
			d		
—		—		0.8	1.0
			N		
			s		
4150.0	0.001 845	4150.0	0.001 845	4150.0	0.001 845
620.1	0.014 16	620.1	0.014 16	620.1	0.014 16
141.7	0.068 63	141.7	0.068 63	141.7	0.068 63
40.34	0.2286	40.34	0.2286	40.34	0.2286
13.03	0.4662	13.03	0.4662	13.03	0.4662
4.47	0.3657	4.47	0.3657	4.47	0.3657
			sp		
5.425	−0.4133, 0.238	5.425	−0.4133, 0.238	5.425	−0.4133, 0.238
1.149	1.224, 0.859	1.149	1.224, 0.859	1.149	1.224, 0.859
			sp		
0.3	1.0, 1.0	0.297	1.0, 1.0	0.297	1.0, 1.0
			d		
—		—		0.8	1.0

without losing too much accuracy. In our earlier study of LiF, very careful tests were required in order to reduce the CPU time to a few days. Similarly, many tests have to be performed to reduce the required CPU time in the case of BN to reasonable values. Second, one needs a strategy to converge the system in all steps of the global exploration: at the beginning of the search, the unit cell has a very large volume, and the atoms are at random positions within the cell, i.e., the configuration is like that in a gaseous state. The total-energy calculation at such geometry has to be converged, and it has to be converged for all the subsequent steps of the simulated annealing procedure. This has to be done in an automatic way since thousands of calculations at successive geometries are performed. Finally, it is a very interesting and important question whether this procedure will find all the very different structure types: the layered and the three-dimensional (3D) structures such as wurtzite and zinc blende.

II. METHOD

The general method consists of several steps: first, a simulated annealing run with a subsequent stochastic quench is

TABLE III. The Hartree-Fock energies (in hartree per 4 f.u.) of the B_K and wurtzite structures, computed with the small basis sets used during the global optimization (basis sets I and II), in comparison with the energy obtained with the basis set used for the local optimization (basis set III). The geometry was fixed at the computed equilibrium geometry of basis set III (Table V).

Structure	Basis set	Total energy
B_k	I	−316.6687
	II	−316.7495
	III	−316.8753
Wurtzite	I	−316.7014
	II	−316.7419
	III	−316.8452

performed to identify possible candidate structures. This is followed by a local optimization based on analytical gradients. Finally, the symmetry and space group are identified. This is repeated many times in order to identify, as large as possible, a set of structure candidates and to obtain some statistics about the structures found.

The details for the BN calculations are described in the following paragraphs. Four boron and four nitrogen atoms were placed at random positions in a large unit cell which was initially cubic with the cell parameter $a=6.23$ Å. This initial volume is computed by first employing the atomic or ionic radii to estimate the total volume occupied by the atoms in the solid state and then multiplying this number by a sufficiently large factor (typically between 3 and 10) to allow the atoms enough freedom to reach any arrangement independent of the initial random placement in the simulation cell. This factor was varied in preliminary calculations, where it was found that choosing a larger volume than the one selected ($6.23\times6.23\times6.23$ Å^3=242 Å^3, which is already by a factor of ~5 larger than the volume of, e.g., the zinc-blende structure) did not lead to significantly different results.

Each simulated annealing run had a length of 12 500 steps, and the initial temperature of 1.00 eV (corresponding to 11 604 K) was reduced to ~0.78 eV at the end of the run. The length is thus somewhat longer than in the case of LiF (Ref. 16) because it is more difficult to approach possible candidate structures in a system with covalent bonds. The simulated annealing was followed by a quench with 5000 steps, i.e., a simulated annealing run with a temperature of 0 eV, which means that only downhill moves are allowed during the quench. The quench thus moves the geometry obtained after the simulated annealing further toward a local minimum. The moves were chosen as moving individual atoms (70%), exchanging atoms (10%), changing the lattice parameters with fixed fractional coordinates (10%), changing the lattice parameters with fixed Cartesian coordinates (5%), and changing the origin (5%, this move is important if the cell parameters change subsequently). No symmetry was prescribed during the simulated annealing and quench runs, i.e., the space group was always $P1$.

A minimum distance between two atoms (given by the sum of the radii of the atoms multiplied by 0.7) was prescribed in order to avoid unrealistic geometries which may lead to numerical instabilities. The radii used were based on tabulated values for atomic and ionic radii, as a function of charge, and on the Mulliken charge computed for the previous configuration. In those moves, which change the lattice constant, the probability of reducing the lattice constant was enlarged to 60% to speed up the reduction in the cell size.

The *ab initio* calculations were performed with the CRYSTAL06 code,[38] which is based on local Gaussian-type orbitals. Two basis sets were used during the simulated annealing runs starting from a $[3s2p]$ basis set for B and N, with the inner $[2s1p]$ exponents as in Ref. 39. In the case of basis set I, additional sp exponents of 0.4 for B and 0.3 for N were chosen, and the outermost exponent of the B $2sp$ contraction

TABLE IV. Total energies of the most relevant structures and statistics. Energies are in hartree units (1 E_h=27.2114 eV) for 4 f.u. A run is considered successful if one of the most relevant structures, as displayed in this table, was found.

		Energy (E_h)			Number of times found	
Name of modification	Space group	LDA	B3LYP	HF	Basis I	Basis II
Hexagonal BN	194	−315.9121	−318.5115	−316.8753	1	2
I-BN	160	−315.9125	−318.5110	−316.8740	11	4
II-BN	187	−315.9123	−318.5109	−316.8739	0	2
Wurtzite	186	−315.9629	−318.4988	−316.8452	8	2
Zinc blende	216	−315.9619	−318.4991	−316.8459	4	2
β-BeO	136	−315.9347	−318.4753	−316.8147	2	1
III-BN	62	−315.8958	−318.4437	−316.7821	4	2
IV-BN	8	−315.8810	−318.4685	−316.8243	6	0
V-BN	9	−315.8707	−318.4569	−316.8138	2	0
VI-BN	14	−315.8075	−318.4085	−316.7594	0	1
Number of successful runs					36 (18.9%)	16 (11.5%)
Number of runs in total					190	139

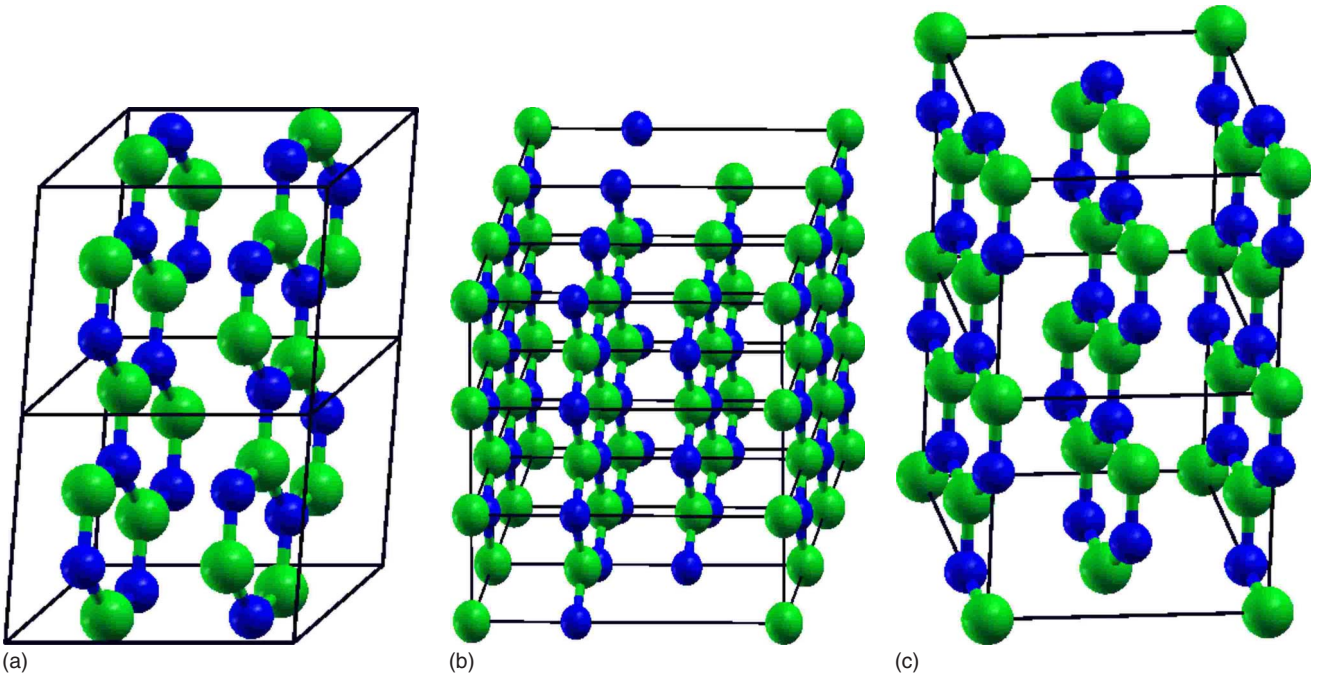

FIG. 1. (Color online) The layered structures found with space groups 194, 160, and 187. Green (light) spheres correspond to boron and blue (dark) spheres to nitrogen atoms, respectively. The lines indicate the unit cells.

(0.4652) was removed. In the case of basis set II, the outer *sp* exponents were chosen as 0.25 for B and 0.297 for N. The basis sets are given in Table II. In the stage of the local optimization, the basis sets used were the $[3s2p1d]$ basis sets from Ref. 32 (basis set III in Table II).

The basis sets during the simulated annealing are therefore chosen slightly different from the ones used in the local optimization (less diffuse functions and no polarization functions) to speed up the global search which is the time-consuming part of the procedure. To test these basis sets, as a preliminary step, the energies of the wurtzite and of the layered B_k structure were computed with various basis sets (Table III). With basis set III, which is used during the local optimization, the B_k structure is more favorable by $\sim 30\ mE_h$, i.e., ~ 0.8 eV $(1E_h = 1$ hartree $= 27.2114$ eV). The smallest basis set I gives preference to the wurtzite structure instead by 33 mE_h (0.9 eV), and basis set II gives preference to the B_k structure by 8 mE_h (0.2 eV). One might

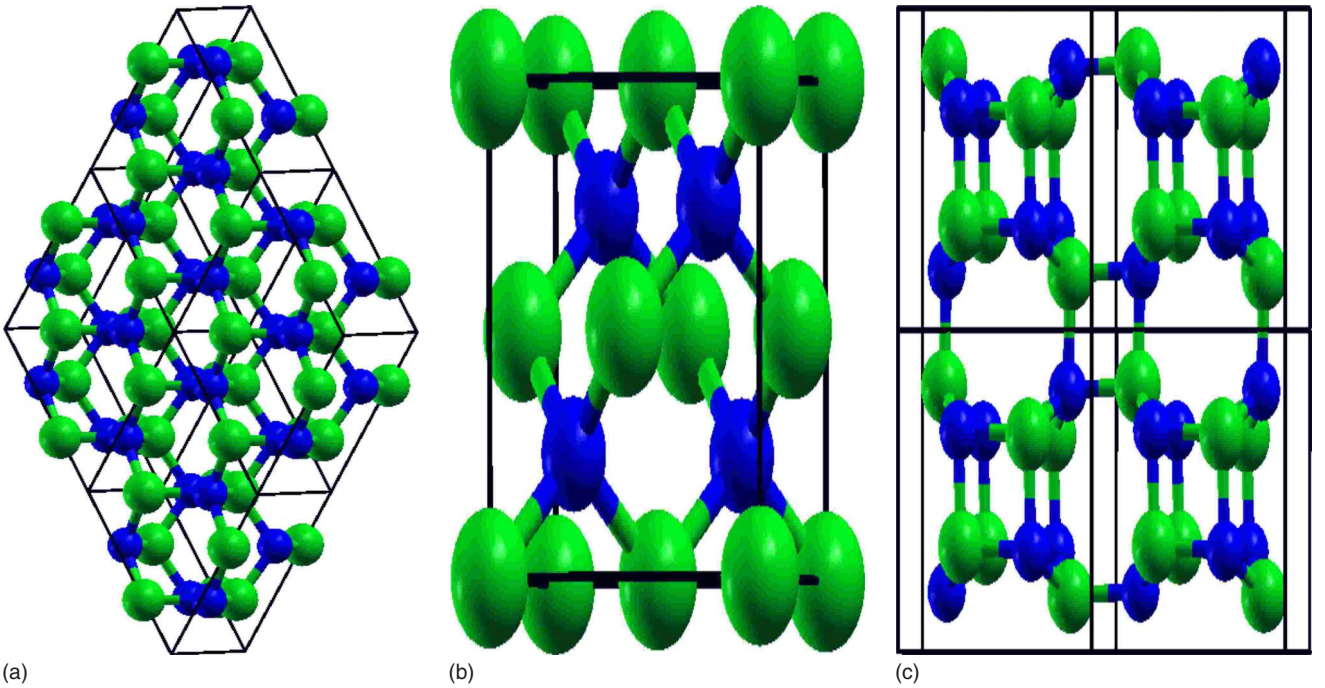

FIG. 2. (Color online) The structures found with space groups 186, 216, and 136.

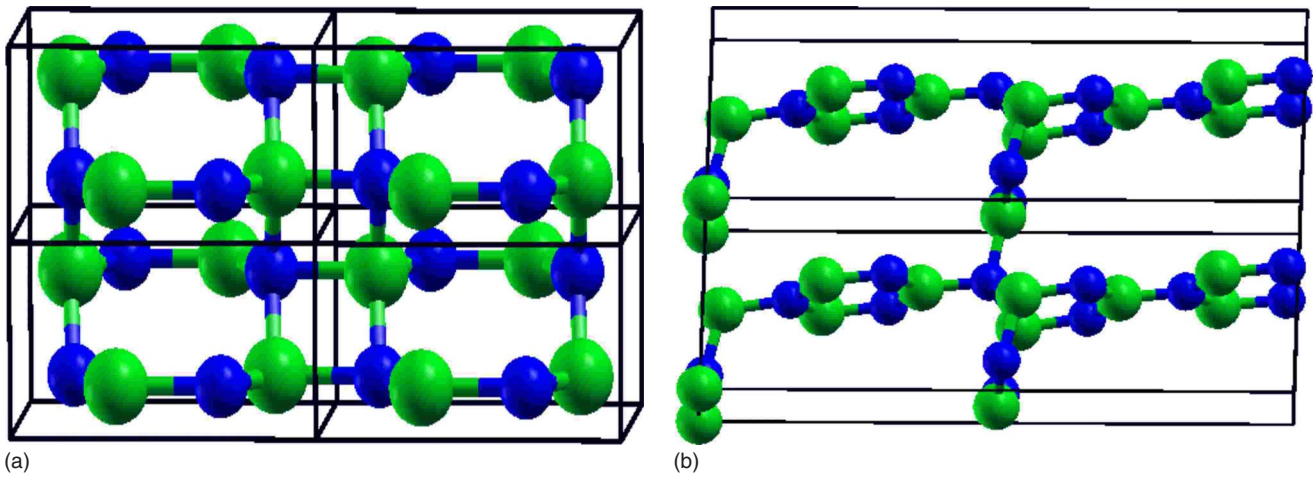

FIG. 3. (Color online) The structures found with space groups 62 and 8.

thus fear that basis set I would not yield the layered structures during the global search; however, this is not the case as will be shown in Sec. III, and there does not seem to be a strong bias due to the basis set. Basis set I is, however, advantageous because calculations are roughly twice as fast as that with basis set II.

Concerning the choice of the *ab initio* method, it has to be taken into account that convergence at a random geometry is necessary during the global exploration stage. As mentioned earlier, the initial geometry has a cell volume approximately five times larger than the experimental volume, and the atoms are randomly arranged. A typical band structure of such geometry is very localized due to the large interatomic distances and completely different from the band structure of the experimental geometry in the solid state. Therefore, convergence is absolutely nontrivial. It turned out that convergence was best achieved with the Hartree-Fock (HF) approach due to the fact that the band gaps are usually very large. Indeed, the band structure and corresponding densities of states display band gaps of ~6 (Hartree-Fock), ~0.5 (B3LYP), and ~0.1 eV [local-density approximation (LDA)] for this *initial* structure. Note that this gap corre-

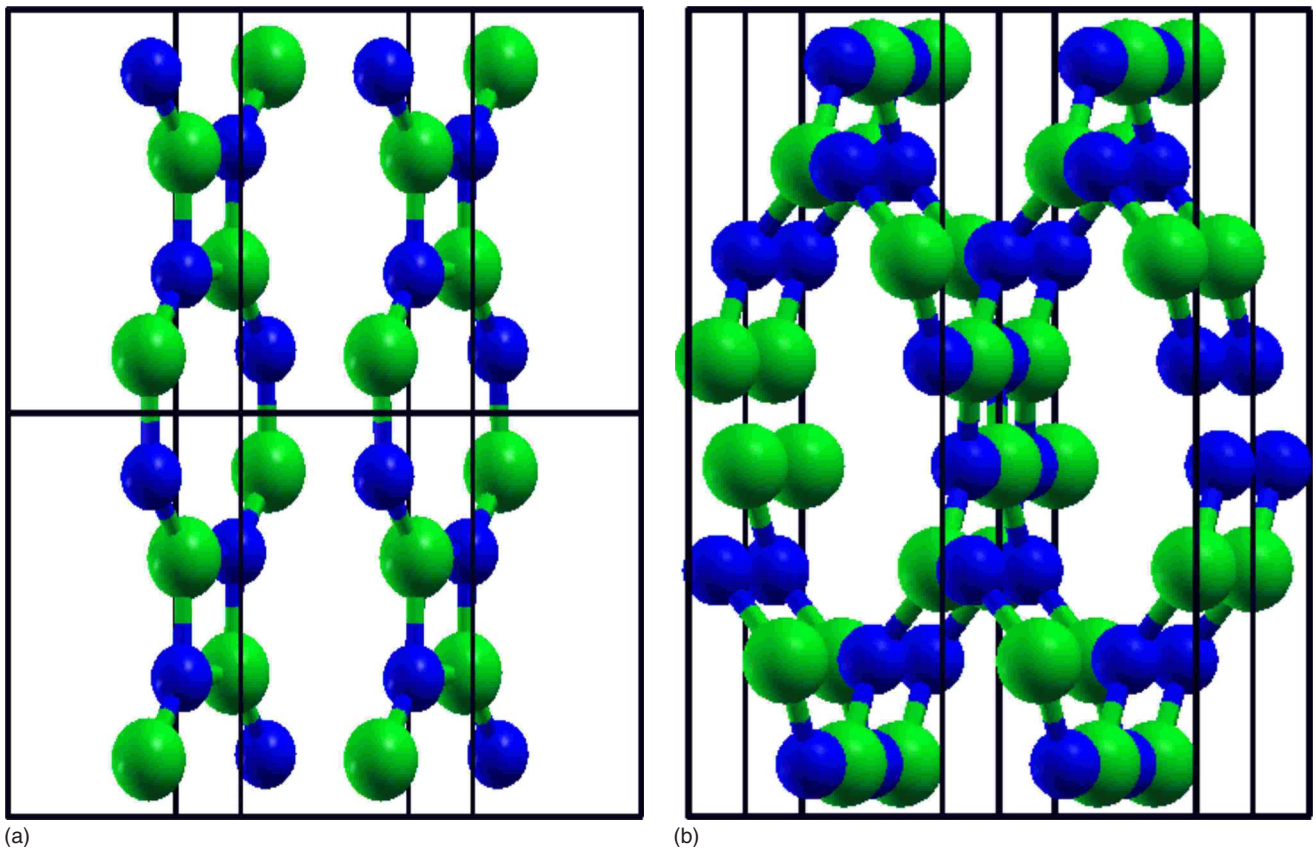

FIG. 4. (Color online) The structures found with space group 14 and 9.

TABLE V. The energetically most favorable structures found.

Space group and modification	Cell parameters and fractional coordinates		
	LDA	B3LYP	HF
194	a=2.50 Å, c=5.88 Å	a=2.51 Å, c=6.40 Å	a=2.50 Å, c=6.43 Å
B_k	B (1/3, 2/3, 1/4)	B (1/3, 2/3, 1/4)	B (1/3, 2/3, 1/4)
Hexagonal BN	N (1/3, 2/3, 3/4)	N (1/3, 2/3, 3/4)	N (1/3, 2/3, 3/4)
160	a=2.50 Å, c=8.72 Å	a=2.51 Å, c=9.56 Å	a=2.50 Å, c=9.69 Å
I-BN	B (0, 0, 0)	B (0, 0, 0)	B (0, 0, 0)
	N (1/3, 2/3, −0.0009)	N (1/3, 2/3, −0.0002)	N (1/3, 2/3, 0)
187	a=2.50 Å, c=5.83 Å	a=2.51 Å, c=6.38 Å	a=2.50 Å, c=6.47 Å
II-BN	B (0, 0, 0)	B (0, 0, 0)	B (0, 0, 0)
	B (1/3, 2/3, 1/2)	B (1/3, 2/3, 1/2)	B (1/3, 2/3, 1/2)
	N (2/3, 1/3, 1/2)	N (2/3, 1/3, 1/2)	N (2/3, 1/3, 1/2)
	N (1/3, 2/3, 0)	N (1/3, 2/3, 0)	N (1/3, 2/3, 0)
186	a=2.54 Å, c=4.19 Å	a=2.57 Å, c=4.23 Å	a=2.55 Å, c=4.21 Å
Wurtzite	B (2/3, 1/3, 0)	B (2/3, 1/3, 0)	B (2/3, 1/3, 0)
	N (2/3, 1/3, 0.3748)	(2/3, 1/3, 0.3750)	(2/3, 1/3, 0.3752)
216	a=3.60 Å	a=3.64 Å	a=3.62 Å
Zinc blende	B (0, 0, 0)	B (0, 0, 0)	B (0, 0, 0)
	N (1/4, 1/4, 1/4)	N (1/4, 1/4, 1/4)	N (1/4, 1/4, 1/4)
136	a=4.38 Å, c=2.54 Å	a=4.43 Å, c=2.56 Å	a=4.41 Å, c=2.55 Å
β-BeO	B (−0.1738, 0.1738, 1/2)	B (−0.1744, 0.1744, 1/2)	(−0.1742, 0.1742, 1/2)
	N (−0.1880, −0.1880, 1/2)	N (−0.1872, −0.1872, 1/2)	(−0.1872, −0.1872, 1/2)
62	a=4.76 Å, b=2.58 Å, c=4.29 Å	a=4.85 Å, b=2.60 Å, c=4.31 Å	a=4.83 Å, b=2.59 Å, c=4.30 Å
III-BN	B (−0.3404, 3/4, 0.0921)	B (−0.3397, 3/4, 0.0912)	B (−0.3399, 3/4, 0.0905)
	N (0.3171, 3/4, 0.1048)	N (0.3211, 3/4, 0.1074)	N (0.3215, 3/4, 0.1078)
8	a=12.95 Å, b=2.50 Å, c=4.33 Å	a=13.08 Å, b=2.51 Å, c=4.39 Å	a=13.03 Å, b=2.50 Å, c=4.37 Å
IV-BN	β=91.7°	β=90.7°	β=90.7°
	B (0, 0, 0)	B (0.0001, 0, −0.0011)	B (0.0002, 0, −0.0008)
	B (0.1998, 0, 0.4266)	B (0.2000, 0, 0.4268)	B (0.2003, 0, 0.4265)
	B (−0.1342, 0, 0.3784)	B (−0.1344, 0, 0.3806)	B (−0.1343, 0, 0.3820)
	B (0.0319, 1/2, −0.4995)	B (0.0319, 1/2, 0.4995)	B (0.0320, 1/2, 0.4998)
	N (−0.0192, 0, 0.3442)	N (−0.0192, 0, 0.3436)	N (−0.0194, 0, 0.3430)
	N (0.0062, 1/2, −0.1562)	N (0.0057, 1/2, −0.1562)	N (0.0051, 1/2, −0.1563)
	N (0.1468, 1/2, 0.4443)	N (0.1471, 1/2, 0.4424)	N (0.1471, 1/2, 0.4409)
	N (−0.1878, 1/2, 0.3908)	N (−0.1876, 1/2, 0.3928)	N (−0.1875, 1/2, 0.3934)
9	a=3.00 Å, b=9.48 Å, c=4.33 Å	a=3.21 Å, b=9.46 Å, c=4.35 Å	a=3.24 Å, b=9.42 Å, c=4.33 Å
V-BN	β=105.1°	β=105.8°	β=106.0°
	B (−0.4996, −0.0652, 0.0001)	B (−0.4991, −0.0657, 0.0004)	B (−0.4985, −0.0658, 0.0006)
	B (0.3780, −0.1931, 0.4920)	B (0.3717, −0.1931, 0.4920)	B (0.3711, −0.1929, 0.4923)
	N (−0.4219, −0.1948, −0.1601)	N (−0.4173, −0.1955, −0.1593)	N (−0.4160, −0.1953, −0.1592)
	N (0.4422, −0.0651, 0.3218)	N (0.4435, −0.0654, 0.3209)	N (0.4423, −0.0653, 0.3202)
14	a=3.17 Å, b=4.90 Å, c=4.93 Å	a=3.44 Å, b=4.92 Å, c=4.94 Å,	a=3.48 Å, b=4.90 Å, c=4.91 Å
VI-BN	β=117.7°	β=115.1°	β=114.3°
	B (0.4963, −0.1429, 0.1385)	B (−0.4998, −0.1428, 0.1413)	B (−0.4992, −0.1427, 0.1417)
	N (0.4984, 0.3443 −0.3418)	N (0.4996, 0.3437, −0.3427)	N (0.4989, 0.3441, −0.3437)

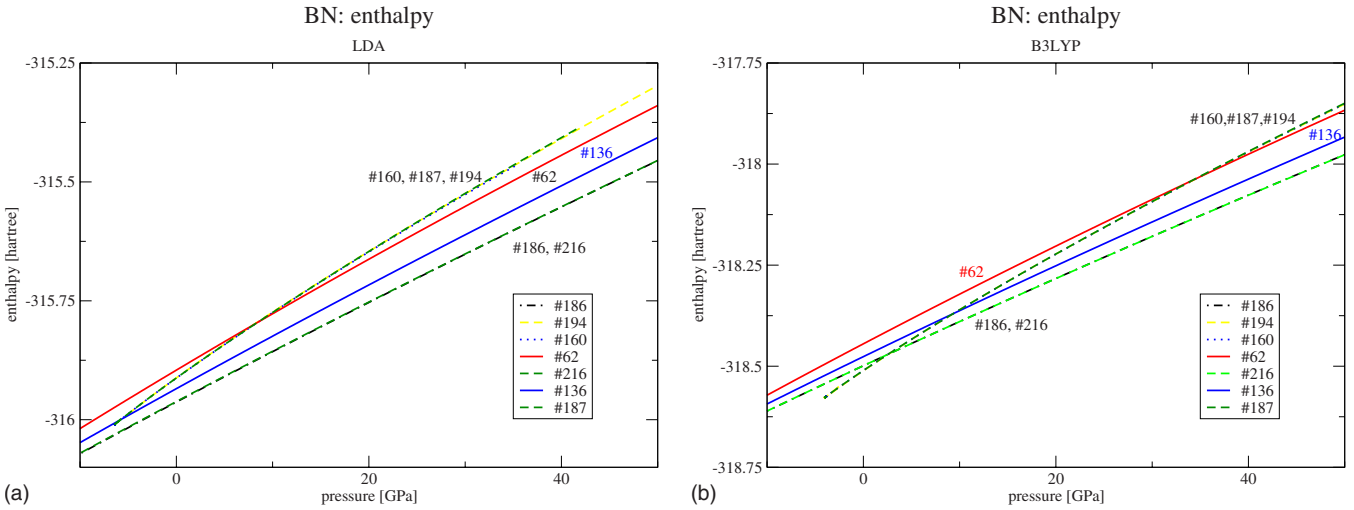

FIG. 5. (Color online) The enthalpy of the most relevant structures at the LDA and B3LYP levels. Structure candidates are labeled by their space groups.

sponds to a random initial structure and is very different from the gap of the final structure; but it is necessary to converge a calculation for this random initial geometry, and for all the geometries subsequently generated, until the end of the simulated annealing and quench. For comparison, calculations with the hybrid functional B3LYP were found to be much more difficult to converge, and a large mixing ratio was required: 90%, in combination with the Anderson mixing scheme, and 35% was sufficient in the case of Hartree-Fock (the mixing ratio is the ratio with which the previous Fock operator is added to the new one, in order to achieve convergence). This leads to many iterations and thus a large CPU time. The LDA was very difficult to converge for random atom arrangements and needed more $\vec{k}$ points and level shifting.

TABLE VI. A comparison of three basis sets for the energetically most favorable structures found.

Space group and modification	Basis set	Cell parameters Å	Energy E_h
		(LDA)	
194	III	a=2.50, c=5.88	−315.9121
Hexagonal BN	IV	a=2.51, c=6.24	−315.9556
	V	a=2.51, c=6.18	−315.9659
160	III	a=2.50, c=8.72	−315.9125
I-BN	IV	a=2.51, c=9.27	−315.9562
	V	a=2.50, c=9.19	−315.9668
187	III	a=2.50, c=5.83	−315.9123
II-BN	IV	a=2.51, c=6.18	−315.9564
	V	a=2.50, c=6.12	−315.9672
186	III	a=2.54, c=4.19	−315.9629
Wurtzite	IV	a=2.54, c=4.19	−315.9884
	V	a=2.54, c=4.18	−316.0035
216	III	a=3.60	−315.9619
Zinc blende	IV	a=3.60	−315.9873
	V	a=3.60	−316.0014
136	III	a=4.38, c=2.54	−315.9347
III-BN	IV	a=4.39, c=2.54	−315.9591
	V	a=4.37, c=2.54	−315.9749
62	III	a=4.76, b=2.58, c=4.29	−315.8958
IV-BN	IV	a=4.79, b=2.58, c=4.29	−315.9216
	V	a=4.76, b=2.57, c=4.29	−315.9366

Interestingly, even for the initial structure consisting of widely spaced, nearly isolated atoms, it was sufficient to use the restricted Hartree-Fock approach, i.e., it was not necessary to take into account spin polarization, which would be the case for a free atom.

The thresholds for integral selection were enlarged from 1×10^{-6}, 1×10^{-6}, 1×10^{-6}, 1×10^{-6}, and 1×10^{-12} to 1×10^{-4}, 1×10^{-4}, 1×10^{-4}, 1×10^{-4}, and 1×10^{-8}, respectively, and the self-consistent-field cycles were stopped when the difference between two subsequent cycles was below 1×10^{-4} E_h. A mesh with $4\times4\times4$ $\vec{k}$ points was used. The error associated with the $\vec{k}$ mesh can be estimated by computing the energy difference when changing the lattice constant, e.g., changing the lattice constant of BN in the zinc-blende structure from 3.7 to 3.6 Å changes the energy by 0.013 68 E_h for four formula units (f.u.) with a $4\times4\times4$ mesh and by 0.014 36 E_h with a $8\times8\times8$ mesh. The associated error with the mesh is thus 0.014 36−0.013 68 =0.000 68 E_h and reasonably small.

The simulated annealing and subsequent quench are the time-consuming parts, and a single run takes the order of one week on a single CPU. The same approach would have been feasible with the B3LYP functional, but at a much higher cost, for the reasons discussed above (around a month instead of one week CPU time). It appeared therefore that it is more reasonable to perform four times as many runs (here, around 329, see Table IV) using the Hartree-Fock approach than with the B3LYP approach where around 80 runs would have been feasible with a comparable total CPU time.

The local optimization is not very time consuming and was done with default parameters for the integral selection

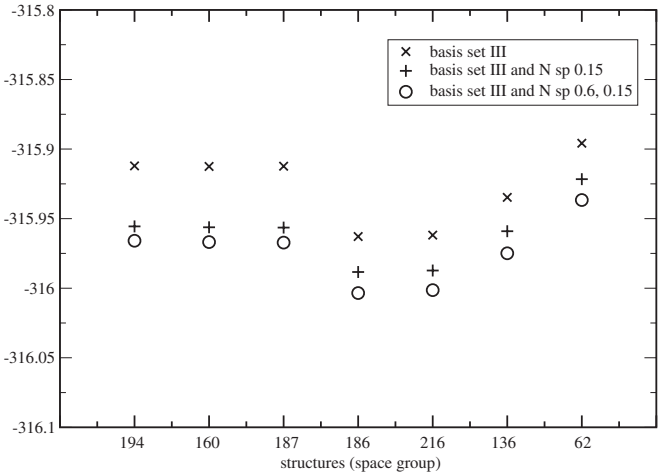

FIG. 6. Total energies for the various structures, in hartree per 4 f.u., for basis sets III, IV, and V at the geometry optimized for each basis set. Structure candidates are labeled by the space group.

and the self-consistent-field cycles. The full geometry optimization can, by now, be routinely performed with analytical gradients[40–44] as implemented in the CRYSTAL06 release. The local optimization, starting from the structure after the quench, was done both at the HF level and at the LDA level; in nearly all the cases, the resulting final minimum structures turned out to be the same. In addition, for these final structures, a B3LYP optimization was also performed in order to compare Hartree-Fock, B3LYP, and LDA. The basis set used was basis set III in Table II. In addition, in the Appendix, larger basis sets were tested for comparison.

The symmetry was analyzed with the program KPLOT (Ref. 45) where algorithms are implemented to find the symmetry and space group.[46,47] For the most important structures, the enthalpy was computed in order to investigate the pressure dependence of the phases.

III. RESULTS AND DISCUSSION

The most relevant structures found are displayed in Figs. 1–4, which are visualized with XCRYSDEN.[48] Optimized geometries are given in Table V. First, the experimentally observed B_k structure was obtained (so-called hexagonal boron nitride and space group 194). Two additional layered structures are closely related with space group 160 and 187, respectively. In the B_k structure, sheets are made of edge-connected six-membered rings of three boron and three nitrogen atoms in alternating sequence (see Fig. 1, left). The neighboring sheets are stacked vertically below and above with alternating atoms (i.e., N sits vertically above B and vice versa; the stacking order is *ABAB*). In space group 160, the same sheets are formed but only three atoms have neighbors in the layer above and the other three atoms have neighbors in the layer below [the stacking order is *ABCABC*, i.e., like in rhombohedral BN (Ref. 25)]. The structure with space group 187 has stacking order of *ABAB*, where again three atoms have neighbors vertically above and below in the next layer. These three layered structures have a very similar total energy, and also the enthalpy as a function of pressure looks very similar (see Fig. 5).

The wurtzite structure is displayed in Fig. 2(a). The zinc-blende structure is displayed in Fig. 2(b) and has a similar energy as the wurtzite structure. At zero pressure, the energies of the wurtzite and zinc-blende structures are comparable to that of the layered structures in Fig. 1.

The structure with space group 136 has six-membered rings (three B and three N—alternating) as well as rings with four (two B and two N) atoms. This leads to angles close to 90° and a less favorable energy [see Fig. 5(a)]. This structure corresponds to the β-BeO-type,[49] which demonstrates that the method presented gives reasonable low-lying structure candidates: as Be has one electron less than B and O has one electron more than N, it makes sense that the β-BeO structure is also found as a candidate structure for BN. Under ambient conditions, BeO crystallizes in the wurtzite structure, and the β-BeO structure is found as a high-temperature phase.[49]

The structure with space group 62 has four- six- and eight-membered rings [see Fig. 3(a)]. The topology is similar to the one of the aluminum network in the $SrAl_2$ structure under ambient pressure (space group 74, Imma).[50] One has to replace one aluminum atom with boron, the neighboring one with nitrogen, and discard the strontium. This is reasonable, as the two aluminum atoms obtain two electrons from strontium and thus have eight valence electrons together, i.e., the same number of valence electrons as one boron and one nitrogen atom together. The structure with space group 14 consists of layers—each of them consisting of rings with four or eight atoms. Finally, two structures with relatively large channels (i.e., large regions in the unit cell without atoms) were found with space groups 8 and 9, respectively.

The geometries are in reasonable agreement with the available experimental data in Table I. The computed cell parameter a and the interlayer distance are approximately constant for the layered structures with only six-membered rings (with space groups 194, 160, and 187); this is also observed in the experiment when comparing the B_k and the rhombohedral structure.

Total energies and statistics are given in Table IV. The five energetically lowest-lying structures found were the layered (space groups 194, 160, and 187) and the wurtzite and zinc-blende structures. At zero pressure, LDA favors wurtzite and zinc blende (by 0.05 E_h per 4 f.u.), whereas B3LYP (by 0.01 E_h) and Hartree-Fock favor the layered structures. This is in reasonable agreement with other calculations, e.g., Ref. 36 and references therein gives the layered structure by $\sim$0.06 eV/atom (0.02 E_h per 4 f.u.) higher than the wurtzite and zinc-blende structures. Also, the zinc-blende and wurtzite structures are nearly degenerate and similarly the hexagonal and rhombohedral structures. These results are stable with respect to the choice of the basis set, as calculations with larger basis sets show (see the Appendix).

Statistics show that the layered structures are frequently found, as well as the 3D structures such as wurtzite or zinc blende. Statistics include all runs where Hartree-Fock energies were used during the simulated annealing. Ten runs were performed, where the B3LYP functional was used during the simulated annealing procedure. In two of these runs,

a good structure candidate was found (wurtzite and the layered structure with space group 160). However, as was mentioned, the B3LYP runs require much more CPU time, and therefore, the runs were mainly performed using the Hartree-Fock approach during the simulated annealing. In total, about 16% of the runs gave one of the structure candidates in Table IV. The other runs yielded either no good structure candidates (such as "amorphous" structures) or only energetically very unfavorable structures.

When pressure is applied, the lower coordinated structures become less favorable, which is in agreement with the rule that the coordination number increases with pressure—see, e.g., Ref. 51. The enthalpies are displayed in Fig. 5 for LDA and for B3LYP, respectively. Interestingly, in the case of B3LYP the layered structures are favorable at zero pressure, with wurtzite and zinc blende becoming favorable at a pressure of ~3 GPa.

IV. CONCLUSION

It was shown that structure prediction based on simulated annealing and using *ab initio* energies during both the global and local optimizations is feasible for a covalent system such as boron nitride. This is a significant extension of the previous work[16] where this approach was shown to be feasible for an ionic system. Covalent systems are more difficult to study as covalent bonds need to be established between the neighbors and convergence problems are more severe in this case. Three layered structures, the wurtzite and zinc-blende structures, a structure of the β-BeO-type, and four other favorable structures were found. Applying pressure leads to a preference of the higher coordinated structures.

ACKNOWLEDGMENT

We would like to thank D. Proserpio (Milano) for a valuable discussion.

APPENDIX: LARGER BASIS SETS TO EXTRAPOLATE THE BASIS SET LIMIT

In the present work, the main task is to compute the energy differences between various structures. Besides the functional, the choice of the basis set has an influence on these results. In order to investigate this in more detail, the basis set used for the local optimization was further enlarged, and the total energies were computed for the most important structures. Here, enlarging the basis set means including more diffuse functions. It turned out that this was only possible for the nitrogen atom, whereas more diffuse functions on boron led to linear dependence problems. Therefore, in a first step, one *sp* shell with exponent 0.15 was added to the nitrogen basis set III in Table II, which resulted in a $[4s3p1d]$ basis set for nitrogen (basis set IV). In a second step, two *sp* shells (with exponents 0.15 and 0.6) were added to the nitrogen basis, i.e., a $[5s4p1d]$ basis set was obtained (basis set V). Note that these basis sets work reasonably well at zero pressure but numerical instability sets in with compression, i.e., enthalpies (as in Fig. 5) could only be obtained up to a relatively small pressure.

A geometry optimization was performed with these basis sets. The results are displayed in Table VI. It becomes obvious that the energy differences between the various structures remain essentially constant; the total energy becomes lower with increasing basis set. This is visualized in Fig. 6.

The geometry slightly changes when enlarging the basis set. The most prominent is the change of the *c* axis for the layered structures when the basis set is enlarged. This is due to the weak bonding between the individual layers. However, as a whole, the basis set does not change the relative energies between the structures.

[1] J. Maddox, Nature (London) **335**, 201 (1988).
[2] M. L. Cohen, Nature (London) **338**, 291 (1989).
[3] C. R. A. Catlow and G. D. Price, Nature (London) **347**, 243 (1990).
[4] J. C. Schön and M. Jansen, Angew. Chem., Int. Ed. Engl. **35**, 1286 (1996).
[5] M. Jansen, Angew. Chem., Int. Ed. **41**, 3746 (2002).
[6] S. Kirkpatrick, C. D. Gelatt, Jr., and M. P. Vecchi, Science **220**, 671 (1983).
[7] V. Černý, J. Optim. Theory Appl. **45**, 41 (1985).
[8] J. Pannetier, J. Bassas-Alsina, J. Rodriguez-Carvajal, and V. Caignart, Nature (London) **346**, 343 (1990).
[9] J. Holland, *Adaptation in Natural and Artificial Systems* (MIT, Cambridge, MA, 1992).
[10] *Applications of Evolutionary Computation in Chemistry*, Structure and Bonding Vol. 110, edited by R. L. Johnston (Springer, Berlin, 2004).
[11] A. R. Oganov and C. W. Glass, J. Chem. Phys. **124**, 244704 (2006).
[12] S. M. Woodley, Phys. Chem. Chem. Phys. **9**, 1070 (2007).
[13] A. Nayeem, J. Vila, and H. A. Scheraga, J. Comput. Chem. **12**, 594 (1991).
[14] D. J. Wales and J. P. K. Doye, J. Phys. Chem. A **101**, 5111 (1997).
[15] A. Laio and M. Parrinello, Proc. Natl. Acad. Sci. U.S.A. **99**, 12562 (2002).
[16] K. Doll, J. C. Schön, and M. Jansen, Phys. Chem. Chem. Phys. **9**, 6128 (2007).
[17] J. C. Schön and M. Jansen, Comput. Mater. Sci. **4**, 43 (1995).
[18] Ž. Čančarević, J. C. Schön, and M. Jansen, Chem. Asian J. **3**, 561 (2008).
[19] K. Doll, J. C. Schön, and M. Jansen, J. Phys.: Conf. Ser. **117**, 012014 (2008).
[20] R. S. Pease, Acta Crystallogr. **5**, 356 (1952).
[21] R. H. Wentorf, J. Chem. Phys. **26**, 956 (1957).
[22] F. P. Bundy and R. H. Wentorf, J. Chem. Phys. **38**, 1144 (1963).
[23] F. R. Corrigan and F. P. Bundy, J. Chem. Phys. **63**, 3812 (1975).
[24] A. Mujica, A. Rubio, A. Muñoz, and R. J. Needs, Rev. Mod. Phys. **75**, 863 (2003).
[25] T. Ishii, T. Sato, Y. Sekikawa, and M. Iwata, J. Cryst. Growth **52**, 285 (1981).
[26] J. Thomas, N. E. Weston, and T. E. O'Connor, J. Am. Chem.

Soc. **84**, 4619 (1963).
[27] *Synthesis and Properties of Boron Nitride*, Material Science Forum Vol. 54-55, edited by J. J. Pouch and S. A. Alterovitz (Trans Tech Publications Ltd, Brookfield, 1990).
[28] R. Haubner, M. Wilhelm, R. Weissenbacher, and B. Lux, in *Structure and Bonding*, edited by M. Jansen (Springer-Verlag, Berlin, 2002), Vol. 102, p. 1.
[29] R. M. Wentzcovitch, K. J. Chang, and M. L. Cohen, Phys. Rev. B **34**, 1071 (1986).
[30] K. T. Park, K. Terakura, and N. Hamada, J. Phys. C **20**, 1241 (1987).
[31] A. Catellani, M. Posternak, A. Baldereschi, and A. J. Freeman, Phys. Rev. B **36**, 6105 (1987).
[32] R. Orlando, R. Dovesi, C. Roetti, and V. R. Saunders, J. Phys.: Condens. Matter **2**, 7769 (1990).
[33] Y.-N. Xu and W. Y. Ching, Phys. Rev. B **48**, 4335 (1993).
[34] N. E. Christensen and I. Gorczyca, Phys. Rev. B **50**, 4397 (1994).
[35] J. Furthmüller, J. Hafner, and G. Kresse, Phys. Rev. B **50**, 15606 (1994).
[36] K. Albe, Phys. Rev. B **55**, 6203 (1997).
[37] G. Kern, G. Kresse, and J. Hafner, Phys. Rev. B **59**, 8551 (1999).
[38] R. Dovesi, V. R. Saunders, C. Roetti, R. Orlando, C. M. Zicovich-Wilson, F. Pascale, B. Civalleri, K. Doll, N. M. Harrison, I. J. Bush, Ph. D'Arco, and M. Llunell, CRYSTAL2006, University of Torino, Torino, 2006.
[39] J. S. Binkley, J. A. Pople, and W. J. Hehre, J. Am. Chem. Soc. **102**, 939 (1980).
[40] K. Doll, V. R. Saunders, and N. M. Harrison, Int. J. Quantum Chem. **82**, 1 (2001).
[41] K. Doll, Comput. Phys. Commun. **137**, 74 (2001).
[42] K. Doll, R. Dovesi, and R. Orlando, Theor. Chem. Acc. **112**, 394 (2004).
[43] K. Doll, R. Dovesi, and R. Orlando, Theor. Chem. Acc. **115**, 354 (2006).
[44] B. Civalleri, Ph. D'Arco, R. Orlando, V. R. Saunders, and R. Dovesi, Chem. Phys. Lett. **348**, 131 (2001).
[45] R. Hundt, KPLOT, University of Bonn, Germany, 1979, Version 9, 2007.
[46] R. Hundt, J. C. Schön, A. Hannemann, and M. Jansen, J. Appl. Crystallogr. **32**, 413 (1999).
[47] A. Hannemann, R. Hundt, J. C. Schön, and M. Jansen, J. Appl. Crystallogr. **31**, 922 (1998).
[48] A. Kokalj, Comput. Mater. Sci. **28**, 155 (2003).
[49] D. K. Smith and C. F. Cline, Acta Crystallogr. **18**, 393 (1965).
[50] G. Cordier, E. Czech, and H. Schaefer, Z. Naturforsch. B **37B**, 1442 (1982).
[51] U. Müller, *Inorganic Structural Chemistry*, 2nd ed. (Wiley, Chichester, UK, 2007).